AD-A054 033 MASSACHUSETTS INST OF TECH LEXINGTON LINCOLN LAB F/G 17/9
SOME RESULTS ON PHASE-CODED WAVEFORMS WITH APPLICATION TO REDUC--ETC(U)
FEB 78 D H PRUSLIN F19628-78-C-0002
UNCLASSIFIED TN-1978-7 ESD-TR-78-30 NL

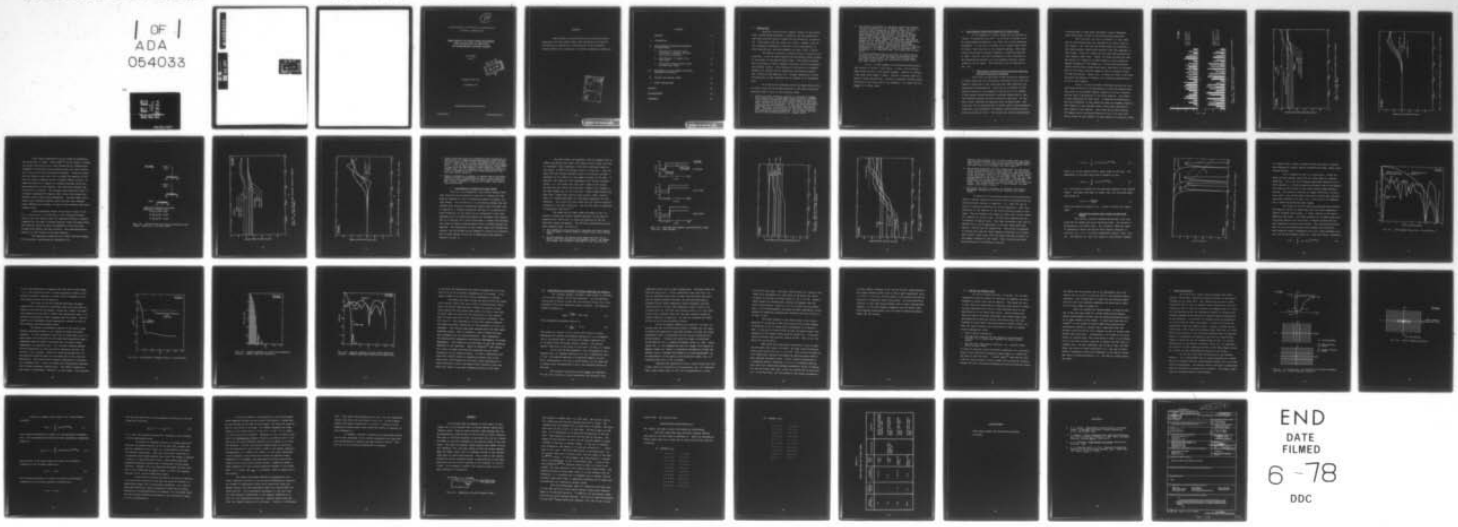

END
DATE FILMED
6-78
DDC

AD No.
DDC FILE COPY

AD A054033

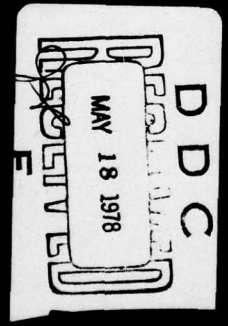

12

MASSACHUSETTS INSTITUTE OF TECHNOLOGY
LINCOLN LABORATORY

SOME RESULTS ON PHASE-CODED WAVEFORMS WITH APPLICATION TO REDUCTION OF INTERFERENCE BETWEEN RADARS

D. H. PRUSLIN
Group 32

DDC
RECEIVED
MAY 18 1978
F

TECHNICAL NOTE 1978-7

28 FEBRUARY 1978

Approved for public release; distribution unlimited.

LEXINGTON MASSACHUSETTS

ABSTRACT

Some results on autocorrelation and cross-correlation properties of binary phase-coded radar waveforms are presented. The results are applied to a consideration of RFI reduction between radars and to questions of clutter suppression capability.

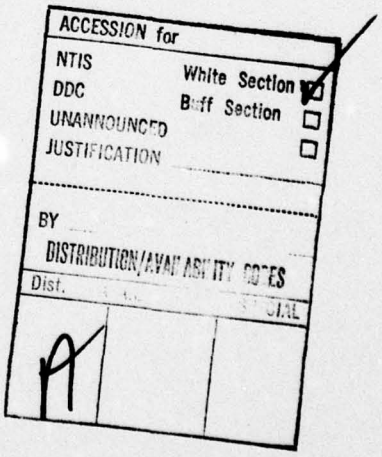

PRECEDING PAGE BLANK-NOT FILMED

CONTENTS

PRECEDING PAGE BLANK-NOT FILMED

I. INTRODUCTION

Recently there has been renewed interest in the properties of phase-coded waveforms, in general, and the possibility that they could be used as a means for RFI reduction, in particular. This report uses the latter as a focus. However, much of the information developed is relevant to the consideration of other applications, and some comments are made in Sec. V below.

The nominal situation to keep in mind as a focus is the following. A set of radars operate multistatically within earshot of each other in the same frequency band. They employ weighted burst waveforms to achieve doppler resolution as well as suppression against clutter. Each subpulse of the burst is a wideband waveform for reasons such as maximizing discrimination potential, improving ECM immunity, etc. Systems operating at L-band and employing 150 MHz subpulses can be thought of as representative.

In trying to say something about how phase-coding could be used to ease the RFI problem implicit in the above situation, questions come to mind in the following areas:

1. Should the phase coding be applied as a modulation within each subpulse, as a phase taper across the burst, or both? In the first instance the phase code becomes the means of pulse compression as well as a possible means of RFI reduction, and thus autocorrelation as well as cross-correlation considerations are important. In the second instance the phase taper will interact with the amplitude taper being used. If coding can be applied at both levels, additional RFI suppression could be possible. In all cases, the key issue is the waveform behavior vs. doppler shift.

2. Two distinct approaches to achieving suppression between radars are possible in the following sense. The first is for each radar transmitter to employ a distinct code. Codes are found by some means such that the cross-correlations satisfy some criterion on peak or average level (average over range extent). The second is for some of the radars to employ a common code. The code selected has a "deep" suppression band over some partial segment of its range extent. By scheduling transmissions among this set of radars, cross-talk is suppressed by the attenuation of the trough during the listening window of a given radar. The potential benefit is greater suppression. A disadvantage is that if the phase code is applied at the subpulse level, the window will be very short.

3. Is there knowledge of how to find sets of codes satisfying given auto- and cross-correlation constraints or how to bound how many exist? Are there design techniques that yield codes having deep attenuation troughs, specified peak levels, etc.?

In Sec. II some examples are presented parametrically that pertain to points 1 and 2 above. In Sec. III we briefly apply these results to the nominal example. Section IV contains a few words about Number 3 above. Section V contains some comments on other applications. Finally an appendix contains specifications of the codes used in the examples. All codes used are binary (0-π) phase codes.

II. SOME EXAMPLES EXHIBITING PROPERTIES OF PHASE CODES

In the examples to follow, range cuts are plotted vs "chips," a normalized time unit. If the code is thought of as an intra-subpulse modulation, this time unit is the compressed pulsewidth. If the code is thought of as a phase taper across the burst, this time unit is the subpulse spacing. When quantities are plotted vs doppler frequency a normalized abscissa is used. Unity on this axis corresponds to the reciprocal of the compressed pulsewidth or of the subpulse spacing, respectively, in the two cases. The difference will be important in Sec. III.

A. "Equivalence" Between Cross-Correlation Functions and Auto-Correlation Sidelobes

Since less is known about cross-correlation properties of phase codes than auto-correlation properties, most codes discussed or tabulated in the literature have some specified auto-correlation characteristics. Since we are interested in both types of functions, the purpose of this section is to examine to what extent cross-correlation functions behave more or less like sidelobe patterns of auto-correlation functions. To this end, we will consider two separate pairs of phase codes. The first pair can be characterized as having "good" auto-correlation properties, with acceptance of whatever cross-correlation properties go along with this. The second pair can be characterized

as having been in some sense "designed" to have reasonable cross-correlation as well as auto-correlation properties.

The first pair is a pair of known[1] 31 chip codes. One has the minimum peak auto sidelobe of any binary code of this length. The other has the minimum peak auto sidelobe of any binary maximal length shift register code (see appendix) of this length. Figure 1-a shows the auto and cross-correlations (zero doppler range cuts). Figure 1-b shows the peak and average values on a range cut of each function vs the normalized doppler frequency of the range cut. On the auto-correlation curves the mainlobe or peak occurring at zero shift is excluded. None of the three functions happen to have an extended trough of high attenuation. Hence, Fig. 1-c shows for each of the three functions the behavior vs doppler of a selected sidelobe which is low at zero doppler.

In Fig. 1-b the noticeable difference between the auto and cross functions is the degradation in peak and average sidelobe level at the greater doppler offsets on the auto function, and the lack of degradation on the cross function. The effect is most pronounced for peak level. A possible rationalization for this difference is that these two codes are somewhat atypical with respect to auto sidelobe level, having been optimized in that regard at zero doppler. Thus, they pop up more strongly off doppler while the cross-correlation level, not being specially chosen at zero doppler, is less sensitive to doppler offset.

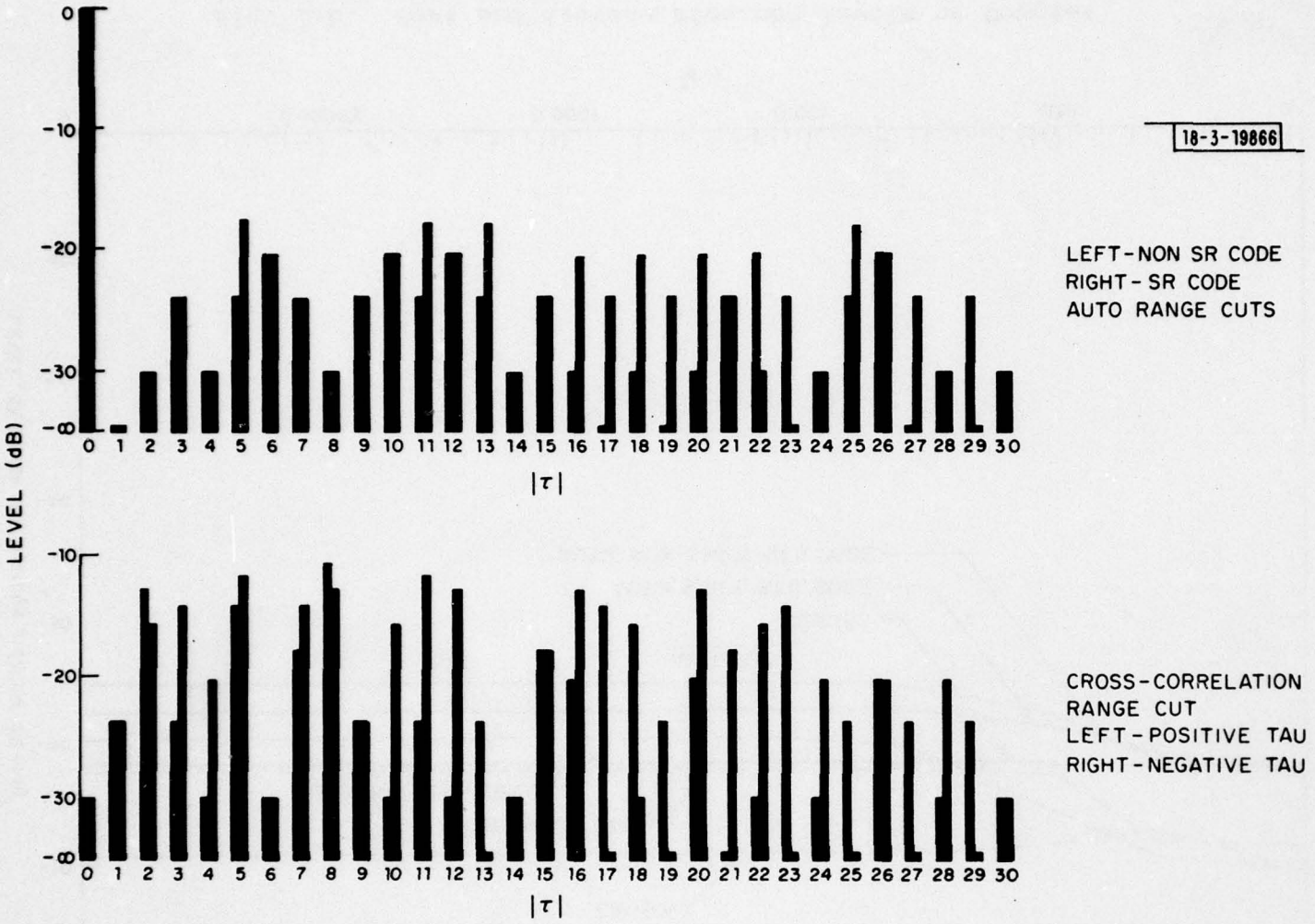

Fig. 1-a. Autocorrelation and cross-correlation zero-doppler range cuts - pair of 31 chip codes.

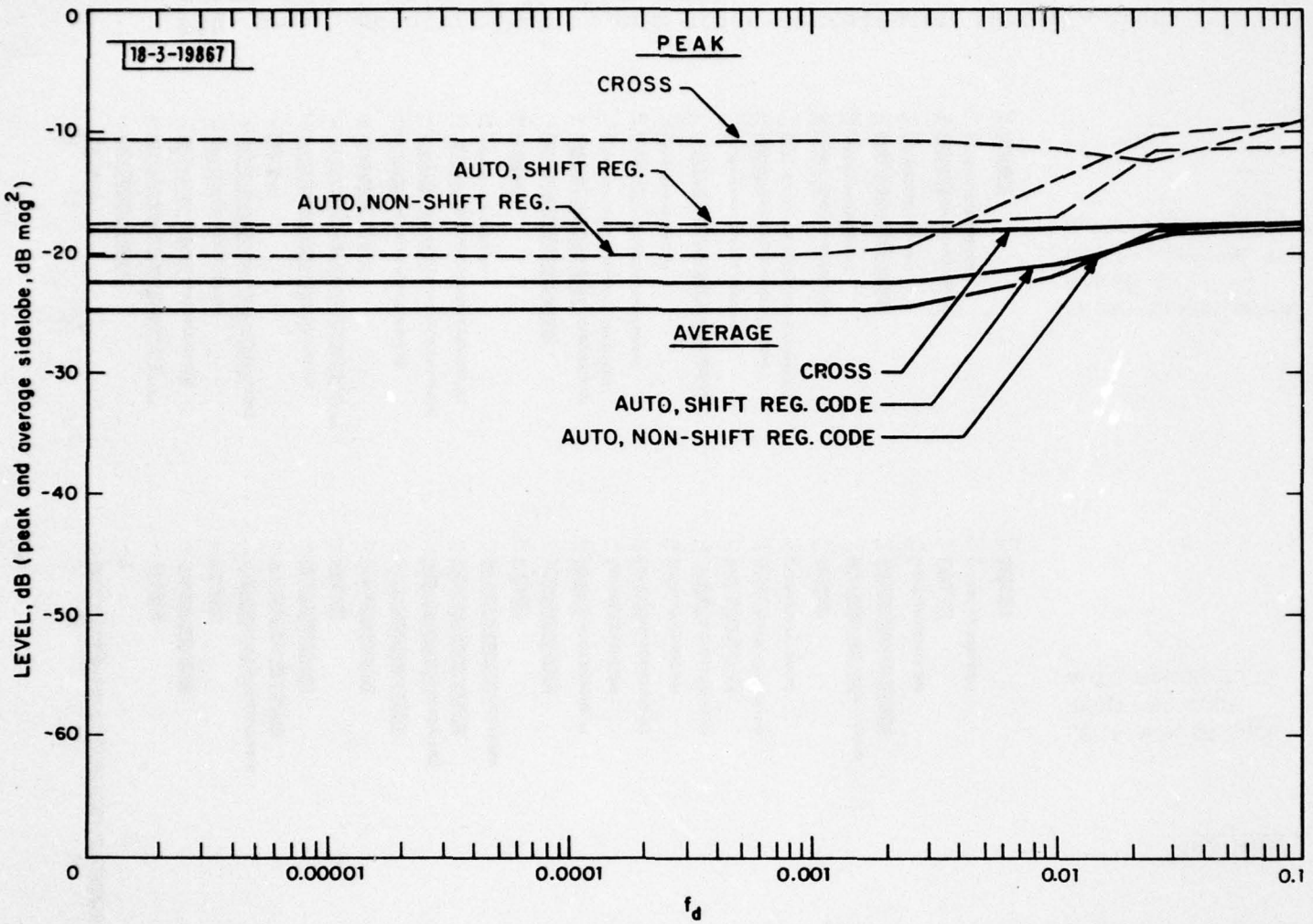

Fig. 1-b. Peak and average sidelobe levels vs Doppler shift - 31 chip codes.

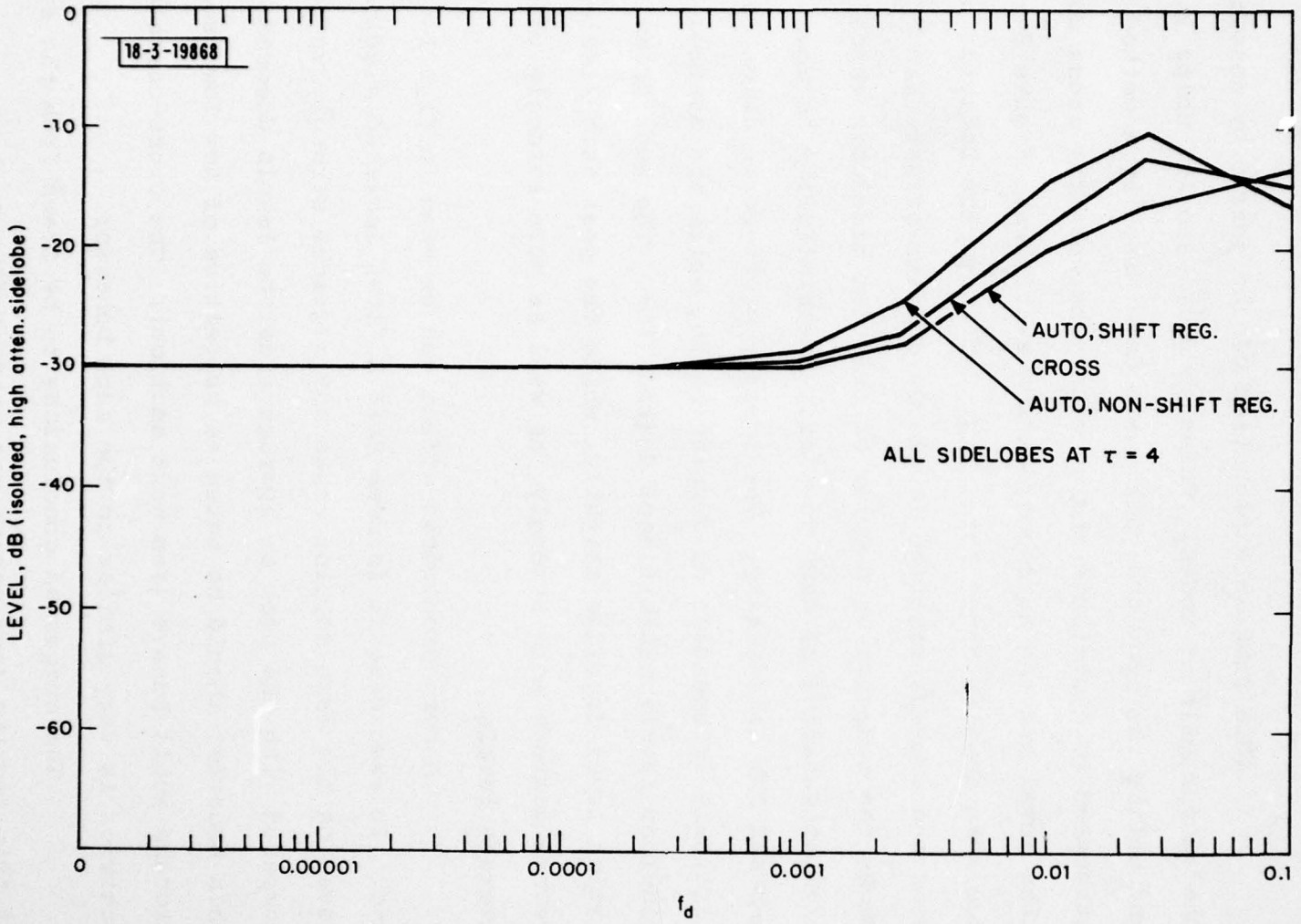

Fig. 1-c. Level of isolated sidelobe vs Doppler shift - 31 chip codes.

This fragile explanation can be jarred by considering the second pair of codes. These codes[2] are 101 chips in length, and unlike the previous pair, were determined by a method which attempted to distribute energy evenly between the cross correlation level and the auto-correlation sidelobes. Figure 2-a shows the zero doppler range cuts, Fig. 2-b shows the behavior of the peak and average sidelobe levels vs doppler offset, and Fig. 2-c shows the behavior vs doppler of selected sidelobes which have high attenuation at zero doppler. The similarity between Figs. 1-b and 2-b is striking. The average cross-correlation level is virtually independent of doppler shift, while the average auto sidelobe levels exhibit some degradation. The peak cross correlation level degrades slightly, while the peak auto sidelobe levels degrade more strongly, as well as more strongly than their average levels.

A more pronounced effect can be seen in Figs 1-c and 2-c. In each case it is seen that a "low" isolated sidelobe level on the zero doppler range cut degrades strongly vs doppler compared with the peak or average sidelobe levels discussed above. This behavior should be taken as suggestive of how low level troughs would behave (see next section). The cross-correlation behavior is very similar to the auto behavior.

The suggested conclusions to be drawn from the examples of this section (and others not presented) are:

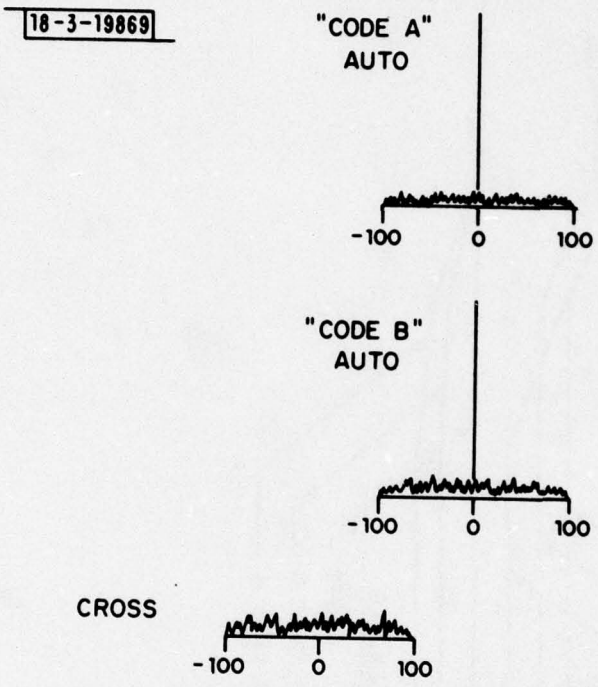

CORRELATION FUNCTION OF TWO BINARY SEQUENCES OF LENGTH N=101;

(A) $\max_k \left|r_1(k)\right|^2 = -21\text{dB}$

(B) $\max_k \left|r_2(k)\right|^2 = -18.5\text{dB}$

(C) $\max_k \left|r_{12}(k)\right|^2 = -16.6\text{dB}$

Fig. 2-a. Autocorrelation and cross-correlation zero Doppler range cuts - 101 chip codes.

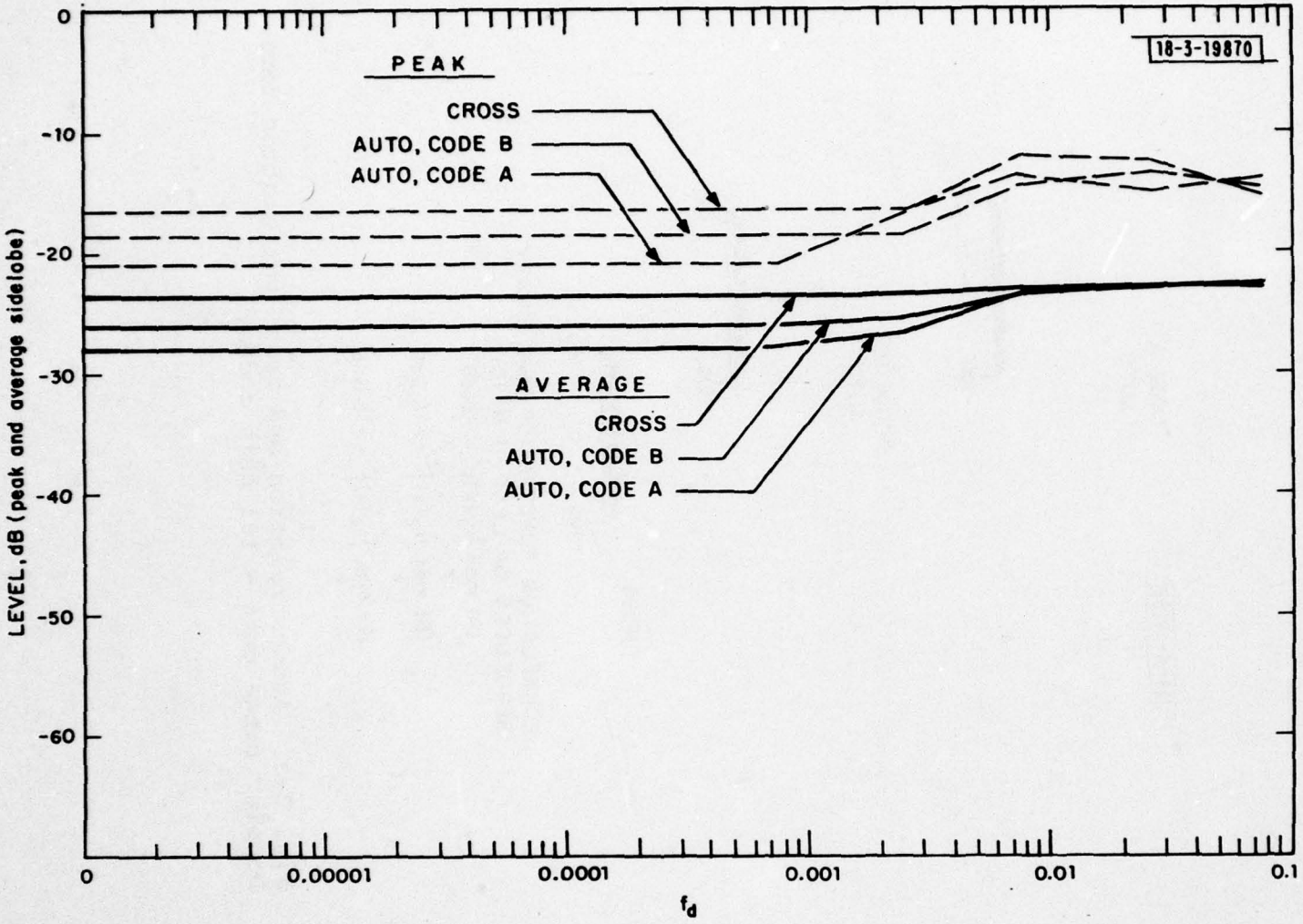

Fig. 2-b. Peak and average sidelobe levels vs Doppler shift - 101 chip codes.

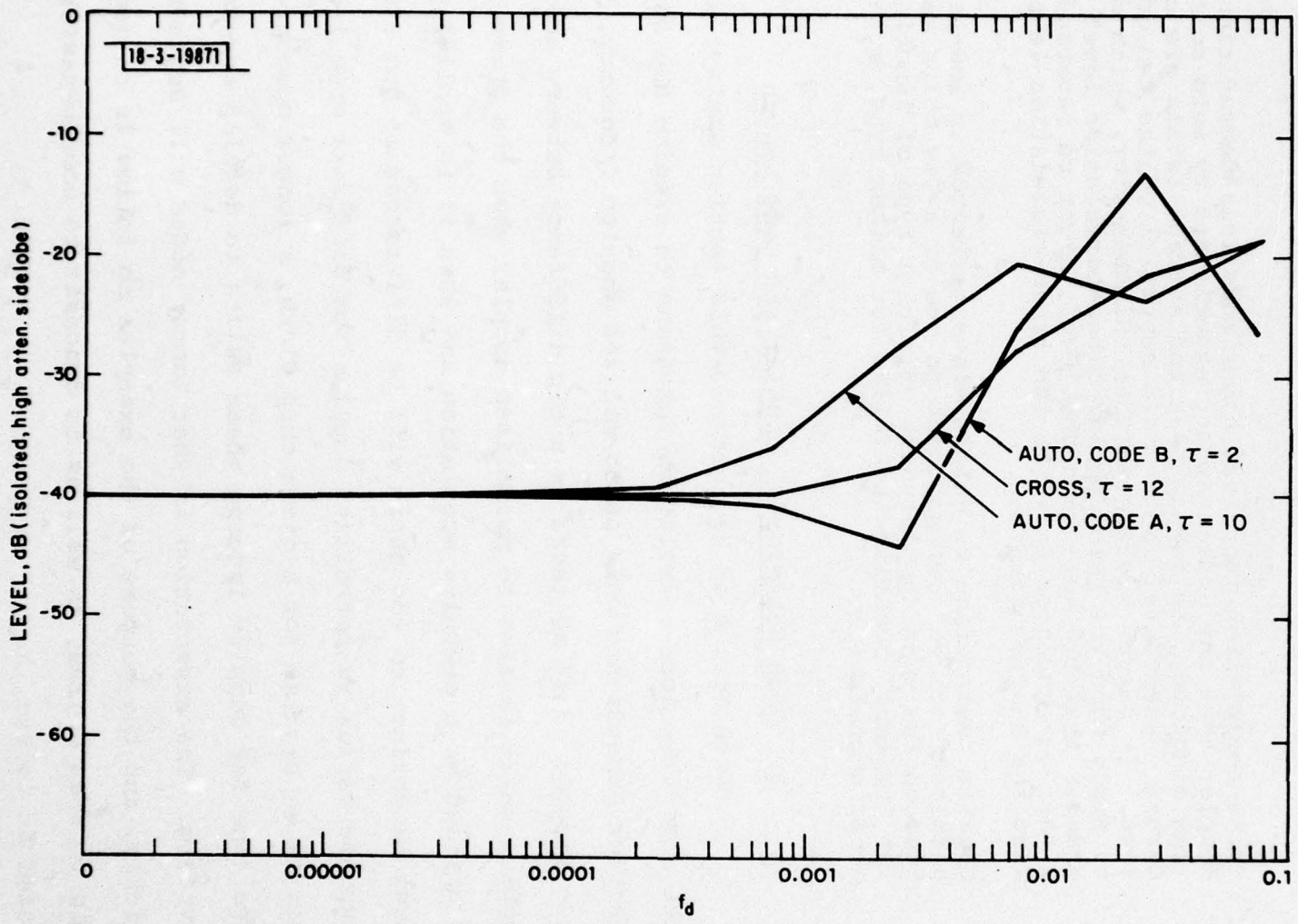

Fig.2-c. Level of isolated sidelobe vs Doppler shift - 101 chip codes.

1. Cross-correlation functions experience less degradation vs doppler than the modest amount experienced by auto correlation sidelobes, as far as peak and average levels are concerned. Peak level is the more sensitive of the two quantities. It can be speculated that this behavior, which seems to apply when the zero doppler cross-correlation level is greater than the auto sidelobe level, might be reversed for a pair of sequences in which the cross-correlation level were the smaller quantity.

2. Greater degradation vs doppler is experienced by low-level sidelobes (those corresponding to one or a few chips residue) on the zero doppler cuts of either type of function. The "typical" behavior is similar for either type, auto or cross correlation.

B. Code Behavior vs Doppler and Code Length

With Sec. A as background, this section employs examples involving auto-correlation functions to examine how code behavior depends not only on normalized doppler frequency, but code length. Just as there is a big difference between how real doppler shift relates to normalized doppler when the phase code is applied as a subpulse modulation and when it is applied as a burst weighting, so too there will be differences in how code response varies vs normalized doppler for different code lengths. This is so because for a given chip width, a longer code provides more time for doppler induced phase shifts to develop across the waveform. The expectation is that longer codes will degrade more quickly, and the purpose of the examples to follow is to quantify this to some degree, as well as to demonstrate some behavior hinted at in Sec. A.

The three codes (see Appendix) used as examples have in common the feature that their zero doppler (auto) range cuts have an "extended" region adjacent to the auto correlation spike at the origin, in which the sidelobe level is "very low." Very low means that the voltage sidelobe levels in the region are small multiples of 1/N, where N is the number of chips in the code. In addition, the codes all have "reasonably low" overall sidelobe levels, i.e., the range cuts look like a spike at the origin sticking out well above the proverbial "rumpled rug" elsewhere. The code lengths are 32, 255, and 1023. These values pretty much span from a length that would be used across a burst (several tens) to a length applicable to a sub-pulse modulation (in the hundreds). The 32 and 1023 chip codes have not received specific attention in the open literature. The 255 chip code is mentioned in Nathanson's text book.[3]

The range cuts of these codes are shown in Fig. 3-a. Figure 3-b shows the overall sidelobe behavior of the codes vs doppler shift, while Fig. 3-c shows the behavior of the low amplitude trench off doppler. The following observations can be made regarding Figs. 3-b and 3-c.

1. The suppression level achievable increases with code length, both in terms of overall peak or average level and of trench depth.

2. At zero doppler, the overall peak levels are near 1/N in power units with average levels somewhat lower. Far enough off doppler the suppression degrades so that the peak and

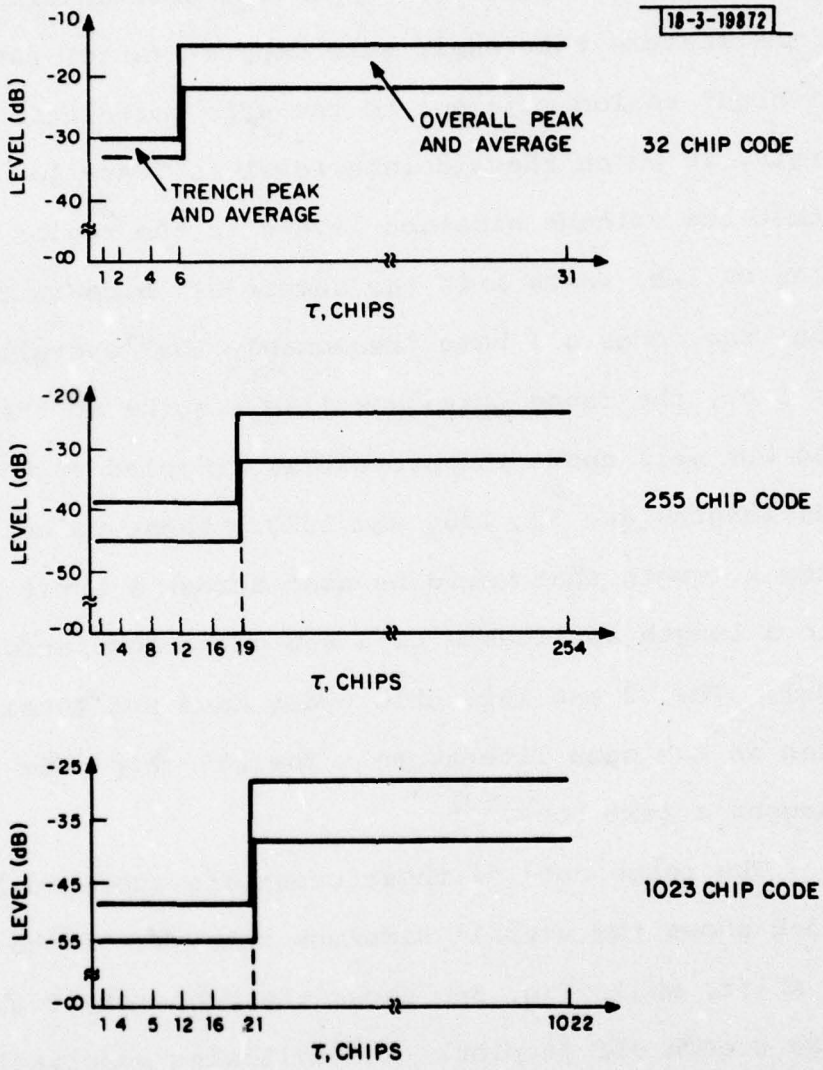

Fig. 3-a. Stylized zero-Doppler autocorrelation range cuts for 3 code lengths.

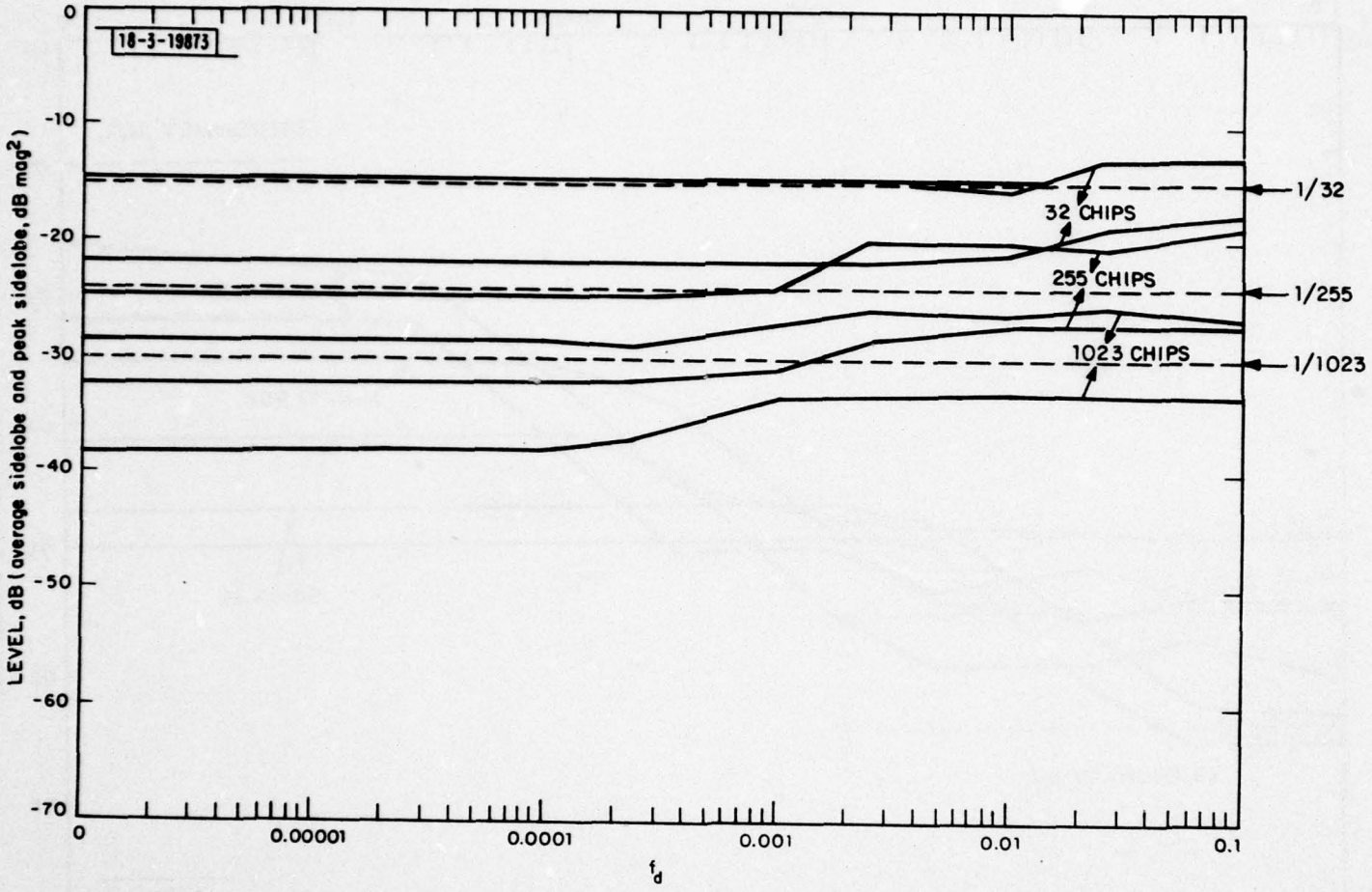

Fig. 3-b. Peak and average autocorrelation sidelobe levels vs Doppler shift for 3 code lengths.

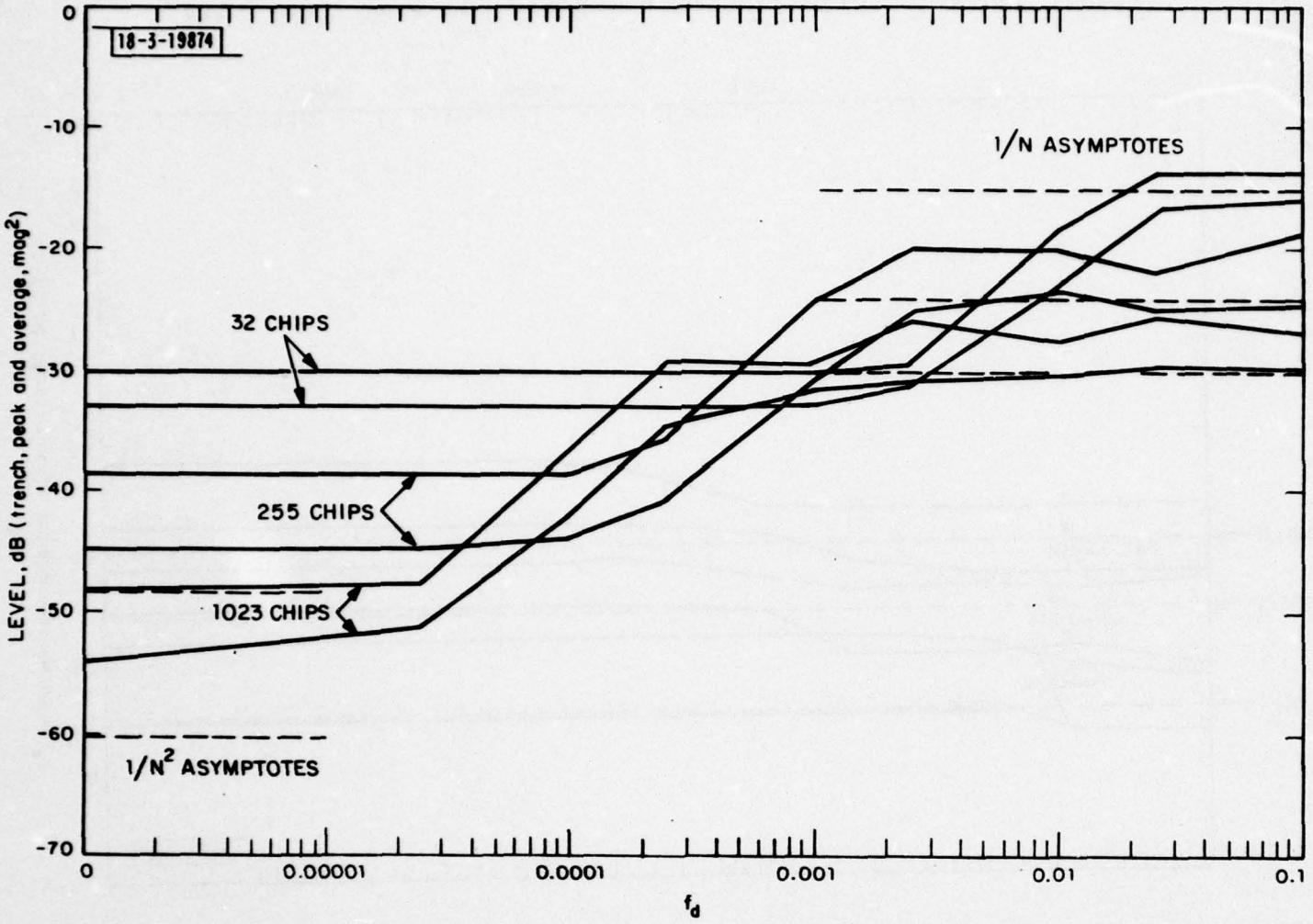

Fig. 3-c. Autocorrelation trench levels, peak and average, vs Doppler shift.

average levels bracket 1/N. Pairs of codes exist for which both auto-correlations and the cross-correlation approximate these levels. If the overall auto levels are pushed lower, the cross level will be higher and vice versa.[2]

3. The minimum achievable non-zero trench level is $1/N^2$ (power units) corresponding to a 1 chip "residue." The definition of the extent of a trench is arbitrary, but typically residue levels of several chips will be included, which is why some of the peak levels in Fig. 3-c are higher than $1/N^2$ (a 4 chip residue appears 12 dB higher on the plot). Off doppler, the degradation is of much greater magnitude and occurs much sooner than the degradation in overall level for a given code length. The trench levels rise to approximately the same values as the overall levels.

4. The longer the code, the sooner it degrades with doppler. Breakpoint frequencies scale about inversely with code length.

In addition to the sidelobe properties discussed above, there is another characteristic which must be considered when the autocorrelation function is important, i.e., when the code is used as a subpulse modulation for pulse compression. That characteristic is the behavior of the auto-correlation spike at zero range. The zero doppler auto range cut looks like a spike riding on a rumpled rug in this case. We have been examining how the rug behaves vs doppler shift. The other degradation that must be checked for is the disappearance of the zero range spike with doppler, leaving only the rumpled rug. This effect corresponds to nothing more than the "basic doppler resolution" of a rectangular pulse N chips long, since the phase code has no effect on the doppler response at zero range. This is easily seen from the definition of the ambiguity function:

$$\chi(\tau,f) = \int_{-\infty}^{\infty} u(t)u^*(t+\tau)e^{-j2\pi ft}dt \qquad (1)$$

where u(t) is the complex signal, phase coded in our case. The dependence of the spike amplitude on doppler is then

$$\chi(0,f) = \int_{-\infty}^{\infty} |u(t)|^2 e^{-j2\pi ft}dt \qquad (2)$$

i.e., the Fourier transform of the magnitude squared of the complex signal. The phase code does not affect this, and the spike amplitude varies as

$$|\chi(0,f)| = \frac{\text{Sin } N\pi f}{N\pi f} \qquad (3)$$

along the normalized doppler axis. Figure 3-d shows this dependence.

C. Interaction Between Phase Codes and Amplitude Tapers

This section contains examples pertaining to the combined use of a phase code and an amplitude taper. We now have in mind working at the burst level. The "original" amplitude taper is employed to obtain the desired burst doppler response, Q-function, etc., i.e., to achieve suppression against "slow" clutter. The question is, what will happen to this doppler response

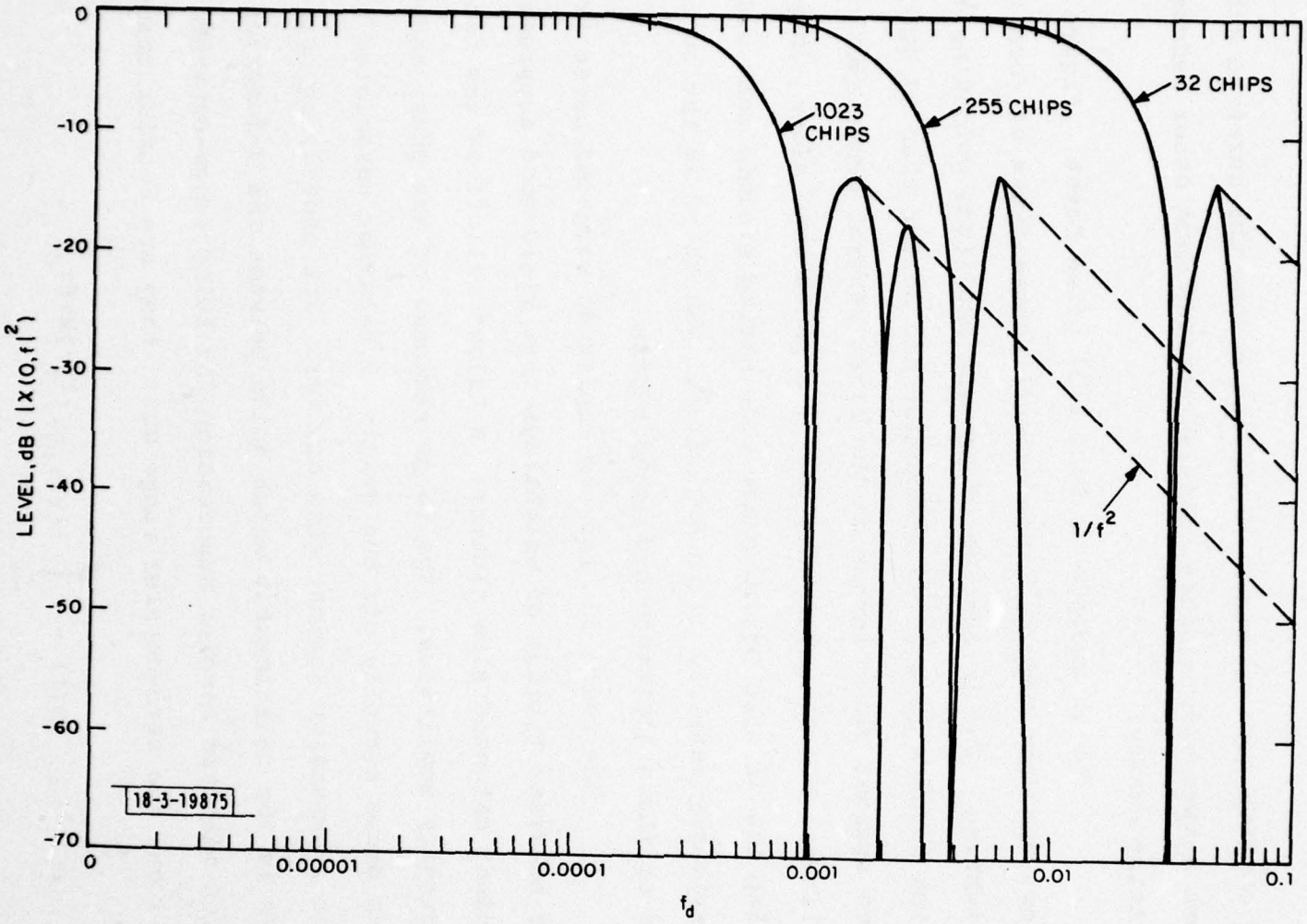

Fig. 3-d. Zero range Doppler cuts for 3 code lengths.

if a phase code or taper is applied across the burst to achieve some suppression against signals received from other radars transmitting nearby?

For an example we take a 31 pulse burst. Figure 4-a shows the zero doppler range cuts for three types of (complex) weighting. One is the use of Hamming amplitude weighting alone, which results in a 30 dB Q-function and better than 60 dB suppression against slow clutter on the first several range ambiguity splines. The second is the use of a phase code alone, in particular the 31 chip Delong phase code having minimum peak sidelobe, previously referred to in Sec. II-B. The third is the combined use of these amplitude and phase tapers.

The range cut for the amplitude weighted burst exhibits the behavior typical of weightings that yield good suppression against extended slow clutter: a "slow" falloff of the near-in ambiguity amplitudes. The range response of the phase coded waveform drops abruptly off the origin, a behavior associated with poor suppression against slow clutter. The underlying principle here is the relationship which holds between the Q-function, which measures doppler suppression for fully range-extended clutter, and the zero-doppler range cut: they are Fourier transforms.

$$Q(f) = \int_{-\infty}^{\infty} |\chi(\tau,0)|^2 e^{-j2\pi f\tau} d\tau \qquad (4)$$

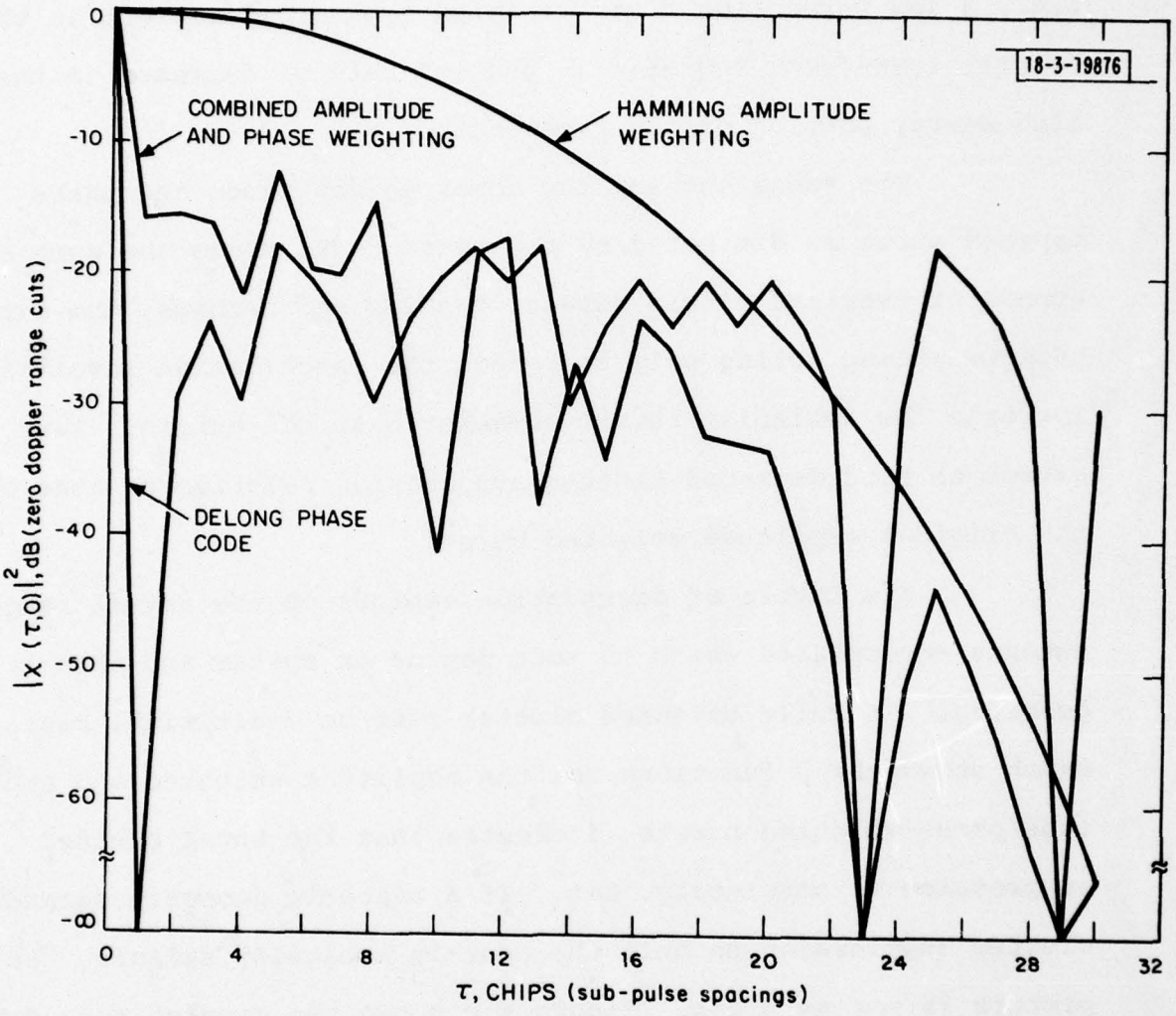

Fig. 4-a. Zero-Doppler Range Cuts, 31 pulse Burst.

To get good suppression at dopplers far from that of the target, i.e., a low Q-function floor or "high frequency" content in the Fourier transform, requires a "gentle" rate of decrease in the high energy portion of the range cut.

The range cut for the combined amplitude and phase tapered burst is dominated by the phase code, since the same sequence of overlaps occurs between 0-chips and π-chips, the amplitude weighting acting only to reduce the cancellation level (i.e., increase the ambiguity level) somewhat near the origin. Thus we expect to find degraded clutter suppression relative to that of the original amplitude weighted burst.

The degree of degradation depends on the actual range extents encountered which in turn depend on system and threat geometry. If fully extended clutter must be dealt with, Fig. 4-b which shows the Q-functions for the amplitude weighted and amplitude/phase weighted bursts, indicates that the burst clutter suppression is completely lost. If a bistatic geometry demands clutter suppression on only the near-in ambiguity splines, the picture is not as bleak. Figure 4-c shows the doppler cuts for the amplitude weighted burst at zero range and on the first two ambiguities. More than 60 dB of doppler suppression is achieved as a response floor. Figure 4-d shows the corresponding responses for the amplitude/phase tapered burst. The doppler response at zero range is undegraded. Equation 2 is the reason. The responses

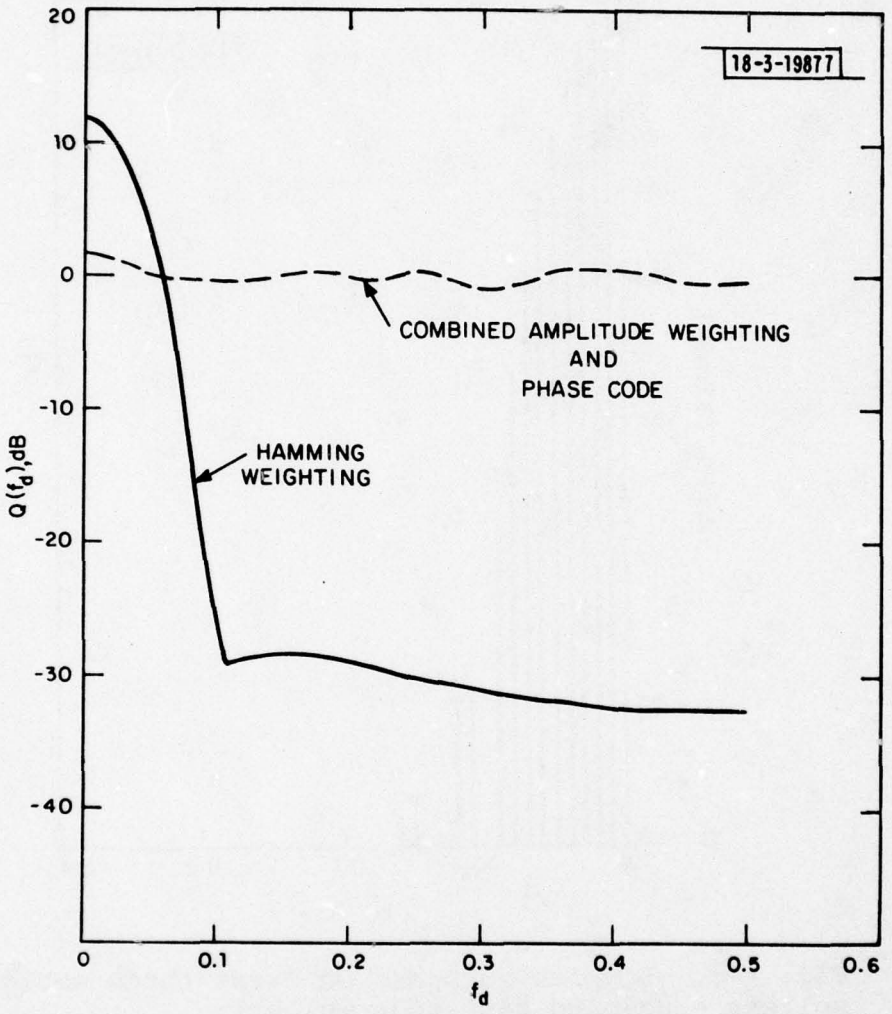

Fig. 4-b. Q-Functions vs Doppler shift, 31 pulse burst.

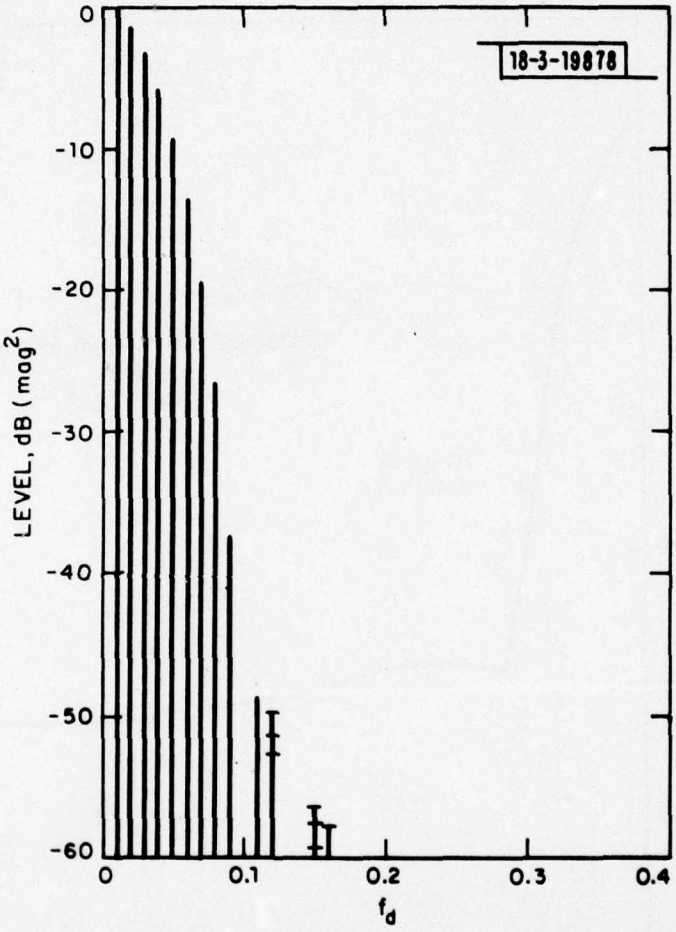

Fig. 4-c. Doppler response on first three ambiguity splines - Hamming amplitude weighting.

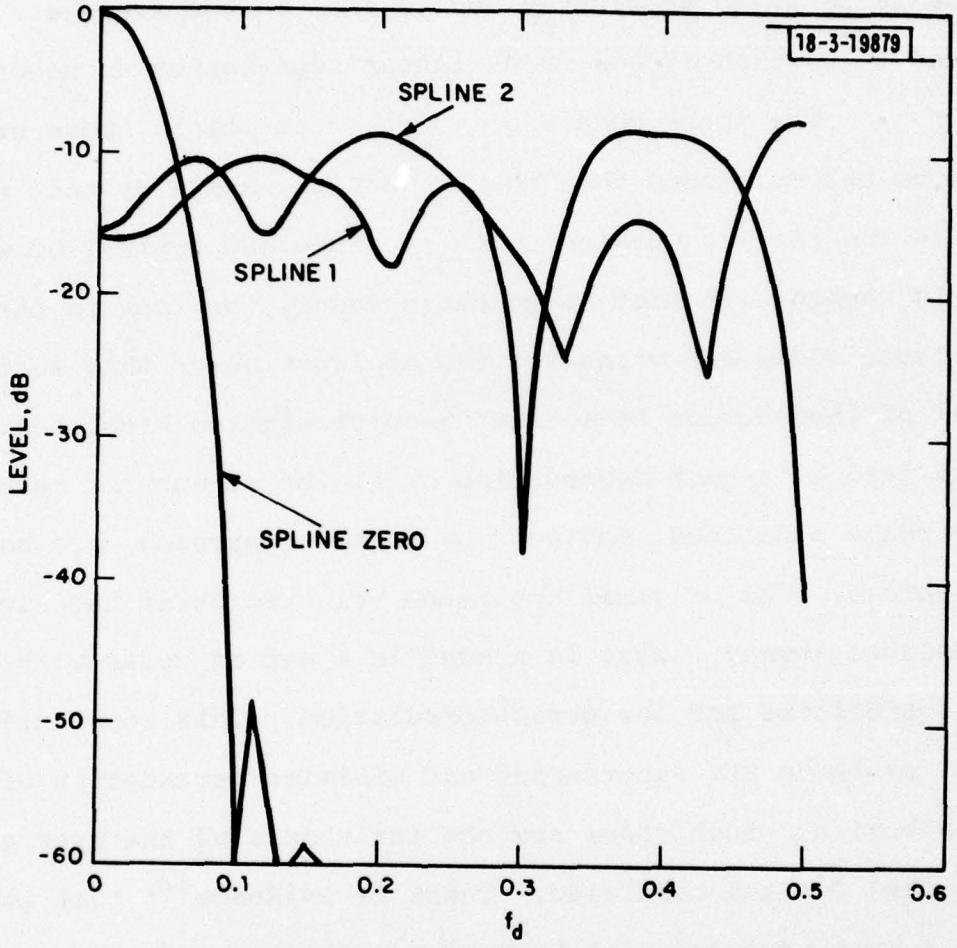

Fig. 4-d. Doppler response on first three ambiguity splines - combined amplitude weighting and phase code.

on the next two ambiguities are greatly degraded but still provide 10 to 15 dB of clutter suppression on the average. It becomes a question of how much clutter suppression is needed.

The phase code used to make the points above was chosen for no better reason than that we had it laying around, really. While the results obtained with it above are typical of what would happen with most known phase codes, the fact is that most of these codes are wrong for the application of this section. Most of these codes have "low" autocorrelation sidelobes. This will lead to a high degradation of the burst doppler response. Low range sidelobes, ambiguities in this approach, are not a requirement. The original amplitude weighted burst has high range sidelobes anyway. What is needed is a set of codes with high auto sidelobes and low cross-correlation. This combination will maximize RFI suppression and minimize degradation of clutter suppression. Such codes are the antithesis of the type generally searched for and tabulated. There is evidence[2] that looking for a pair of codes with high auto sidelobes and low cross-correlation is not fighting nature. If such a combination were found the limiting factor on applying the phase code at the burst level could become the relatively faster degradation of cross-correlation level with doppler shift because of the long chip size (equal to the burst subpulse spacing) of the code.

III. APPLICATION TO THE NOMINAL SITUATION DESCRIBED IN SECTION I

As a nominal example, consider L-band radars at 1000 MHz, a 50 μs burst length, and 150 MHz bandwidth. Let the ambiguous velocity be 10 km/sec to keep the low velocity clutter out of the mainlobe of the first ambiguous doppler response. The ambiguous doppler frequency is:

$$f_{AMB} = \frac{2v_{AMB}}{\lambda} = 66.7 \text{ KHz} \qquad (5)$$

The corresponding subpulse spacing is

$$\Delta = \frac{1}{f_{AMB}} = 15 \text{ μs} \qquad (6)$$

This gives us 3 pulses in 50 μs which isn't much of a burst. Therefore, let's shrink the subpulse spacing to 5 μs, corresponding to an 11-pulse burst, and moving the doppler ambiguity out to 30 km/sec from the primary doppler channel. The nominal doppler resolution of the burst is 1/50 μsec = 20 KHz, or 3 km/sec.

As for the 150 MHz bandwidth, this corresponds to compressing the 5 μs subpulse spacing to 6.7 ns, a compression ratio of 750. The doppler ambiguity or normalized doppler of unity point corresponding to 6.7 ns is 22,500 km/sec, or 750 times the 30 km/sec value corresponding to the 5 μsec subpulse spacing of the burst.

Now consider using phase coding <u>within</u> the subpulses for the joint purposes of pulse compression and isolation from

undesired returns due to other transmitters. The phase codes are then 750 chips long. A giant inferential leap from Figs. 2-b and 3-b indicates that a set of codes "can be found" such that with no doppler offsets involved, the peak auto-correlation sidelobe levels (pulse compression range sidelobes) and peak cross-correlation levels (RFI suppression level) would be 1/N in power units or -28.8 dB, with average levels 5 to 10 dB lower. If the range sidelobe levels are too high, spectral weighting could be applied in some form. We have not examined the effect of this on the cross-correlation levels.

As far as doppler offsets are concerned, one wants to be sure that the auto-correlation doesn't degrade over the range of velocities expected of legitimate targets, and that the cross-correlation level is maintained for RFI returns reflected from moving targets. 7 km/sec will bound the range of velocities we are dealing with, a normalized doppler extent of .0003. Again, taking Fig. 3-b as representing what will happen, this degree of doppler offset will result in negligible degradation of peak and average levels, although the breakpoint is being approached. As for maintenance of the central auto-correlation spike, Fig. 3-d indicates that this is not a problem.

Regarding the approach of using a common phase code with a deep trench and scheduling of transmissions, Fig. 3-c indicates that a peak trench level of $1/N^2$ can be approached as a limit,

-57.5 dB in this case. Allowing a peak residue of 4 chips in the trench will correspond to a peak level 12 dB above this value, or about -45 dB with an average level of -50 to -55 dB. However, these values will degrade more quickly with doppler than the 28.8 dB value above. Using Fig. 3-c as a guide, we can guesstimate a 10-15 dB degradation, bringing the peak suppression corresponding to undesired transmissions reflected off slow clutter up to near -30 dB.

The other problem is the range extent of the trench. Guessing at 10 percent of the code length as what could somehow be achieved, we get 75 chips which corresponds to 10 meters!!! Thus, in this way of doing things we have the absurd result that, assuming all the system timing could be worked out, a listening window 10 meters long would be cleared of RFI. This is not very useful for surveillance.

What about the second basic alternative, that of applying the phase code across the burst? The peak cross-correlation level would now be only 1/11 = -10.4 dB. This could be thought of as an additional isolation achievable by applying phase codes at both subpulse and burst levels. Since .7 km/sec corresponds to a normalized doppler frequency of .23 at 5 μs subpulse spacing, this value will experience whatever degradation occurs vs doppler for the particular code used, if RFI is received off of slow clutter. As we have seen, the big problem is the severe degradation

of burst doppler response on all but the central range ambiguity. The trench approach would yield at best a peak suppression level of $(1/11)^2 = -20.8$ dB, and the extent of the trench would now be measured in kilometers rather than meters. An auto-correlation function of this type would probably lead to nearly maximum degradation of the burst doppler response, and the trench level would degrade significantly over the range of possible doppler shifts for RFI returns.

IV. FINDING THE DESIRED CODES

As can be noticed from Sec. II and Sec. III, we have attempted to make our points by referring to examples that were supposed to typify some kind of behavior. The reason for this is that there are essentially no equations that relate an output waveform characteristic such as a peak sidelobe level to any specification of the phase code itself. Stated another way, there are really no design techniques that produce phase codes with specified properties such as auto-correlation cuts with trenches of given depth, specified overall sidelobe levels, etc. What one finds basically are tabulations of codes (or generational information) which:

1. Were found by enumeration,
2. Satisfy some condition on zero doppler auto-correlation cut only, e.g., lowest peak sidelobe for code of given length.
3. May fall into some special subclass, e.g., maximal length shift register codes.

In terms of pairwise cross-correlation properties, not to mention mutual cross correlation properties among codes in a larger set, one doesn't even find this. A recent paper [2] describes an algorithm for starting with a pair of codes and altering the relation between the auto correlation sidelobes and cross-correlation levels.

The method has some promise and is an improvement over blind search, but it is still a long way from a multi-sequence design technique. Thus finding sets of codes with the desired properties will be a hunt and peck procedure, and there are an awful lot of binary codes of length 750.

Short of a method for finding codes, it would be useful to know how many codes of a given length and satisfying certain requirements on their auto and cross-correlations exist, or at least bounds on this number. A lower bound has been obtained[4] on the number of binary codes having maximum autocorrelation sidelobe no greater than a specified value and maximum cross-correlation level between any pair no greater than another specified value. Unfortunately, for values of the parameters of interest here, this lower bound is zero, so no information on the size of such a code set is gained (the two cases of interest are: low auto sidelobes, say -30 dB or less, 100-1000 chips, any value of cross-correlation; i.e., the use of coding within a subpulse; or: high auto sidelobes, a few tens of pulses, any value of cross-correlation; i.e., the case of coding across the burst).

V. OTHER APPLICATIONS

As we have seen, phase coded waveforms exist which exhibit "extra-deep" suppression regions adjacent to the central response on the range axis. This observation has led to some conjecture that if the low response level extended out from the range axis then it might be possible to encompass most of a clutter distribution within the suppression region by adjusting the waveform parameters and possibly by applying some transformation to the waveform. One scenario of interest would be designation in a tank break-up (TBU) environment, in which the clutter has significant range and doppler extent. Figure 5-a shows qualitatively what a TBU clutter distribution might look like at a time when a surveillance or bulk filtering waveform would be employed. Figure 5-b represents the ambiguity function of a hypothetical signal in which the sort of response shown in Fig. 3-a extends indefinitely in the doppler direction, while Fig. 5-c represents the rotation of this response function in the range-doppler plane as a result of some transformation applied to the signal.

Let us deal first with the rotation of the response function. It is conceivable that in some situations the rotated form of a response function could provide a better fit to a given clutter distribution. The question here is how must a phase-coded signal be modified to produce such a rotation. The answer comes from the following general relationships.

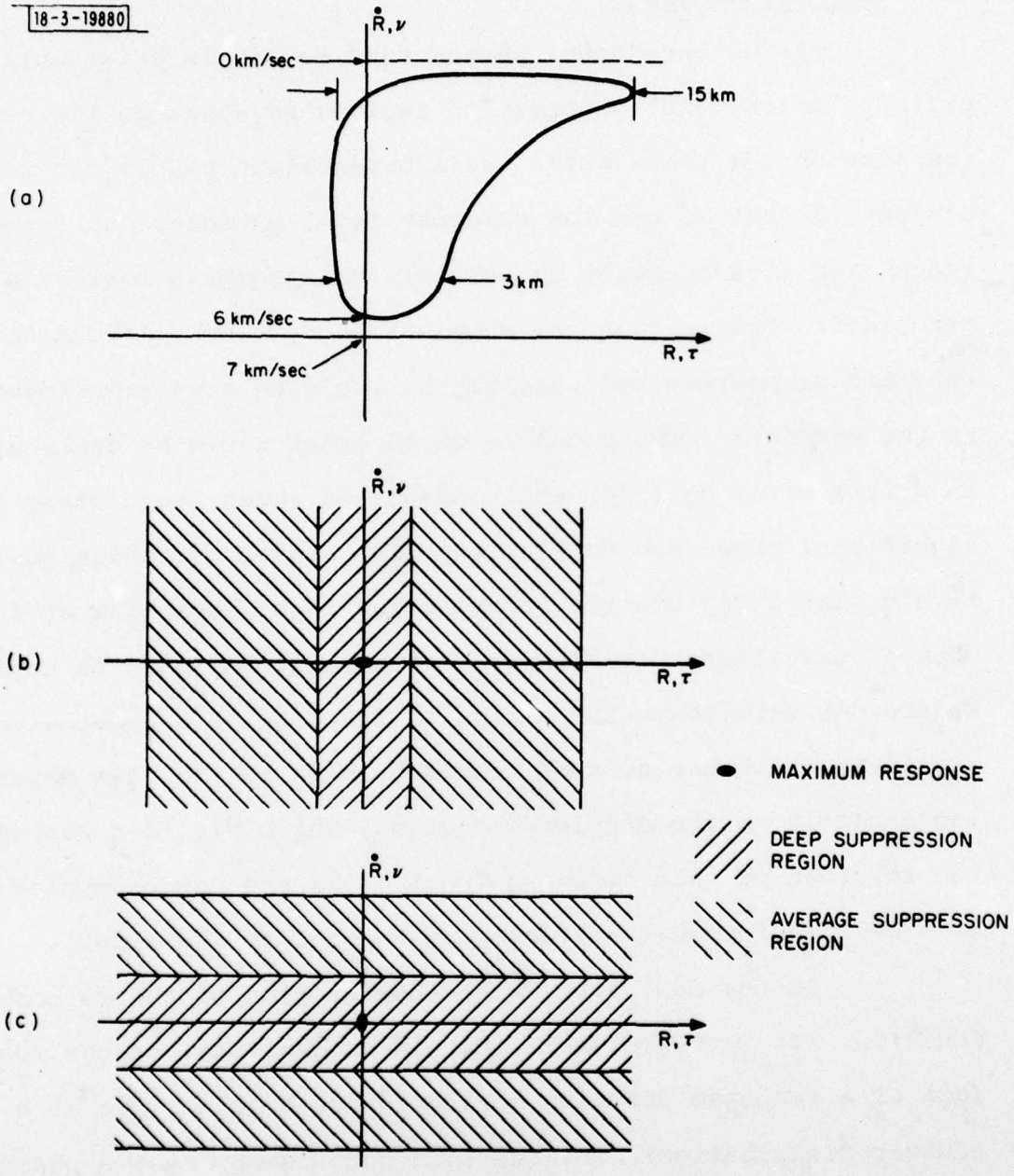

Fig. 5. (a) Clutter map, (b) Hypothetical waveform response function, (c) Rotated response function.

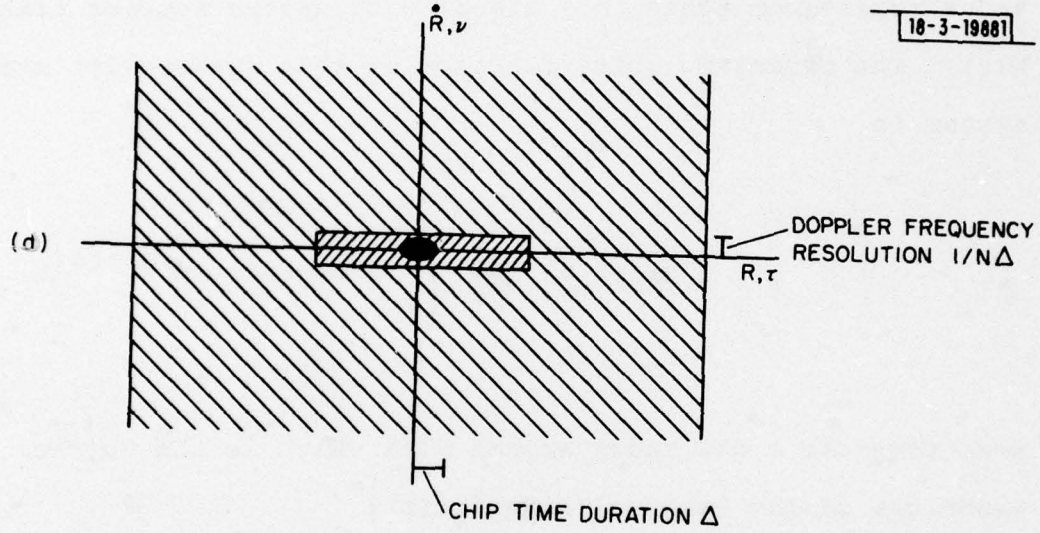

Fig. 5-d. Actual response function.

Consider a complex radar signal x(t), having Fourier transform

$$X(f) = \int_{-\infty}^{\infty} x(t)e^{-j2\pi ft}dt \qquad (7)$$

and a receiver matched to a signal w(t) having Fourier transform W(f). The cross-ambiguity function of this (generally) mismatched system is

$$\chi_{xw}(\tau,\nu) = \int_{-\infty}^{\infty} x(t)w^*(t+\tau)e^{-j2\pi ft}dt \qquad (8)$$

Next consider a new radar signal y(t) which is the Fourier transform of the original signal x(t):

$$y(t) \approx X(t) \qquad (9)$$

and a receiver matched to a signal v(t) which is the Fourier transform of the original weighting function w(t):

$$v(t) = W(t) \qquad (10)$$

One can then show that the cross-ambiguity function for the new signal pair satisfies

$$|\chi_{yv}(\tau,\nu)| = |\chi_{xw}(\nu,-\tau)| \qquad (11)$$

i.e., that the response functions are related by a 90° rotation in the range-doppler plane.

To rotate the response function of a phase-coded waveform and its matched receiver by 90° we must then transmit the Fourier transform of this signal as a time waveform, and match the receiver accordingly. What does the Fourier transform of a "typical" phase-coded waveform look like? The answer in general is that it is characterized by both a continuously amplitude modulated magnitude function and a continuously varying phase function. Remember that this magnitude and phase function would have to be transmitted vs time in order to rotate the response function of the related phase-coded signal.

We see that to achieve any benefit accruing to rotation in a particular situation we must pay the price of trading in a phase-coded signal with its desirable properties, viz, lack of amplitude modulation, ease of generation, simplicity of phase modulation, straightforwardness of receiver, on a new model which has the converse properties and makes a very unattractive candidate for implementation.

Let us now return to the question of fitting the phase-coded response function to the clutter distribution. Assume that we are considering the same 32 chip signal, for which the range extent of the trench is ± 6 chips. To roughly encompass the range extent of the clutter let $6\Delta = 6$ km, or $\Delta = 1$ km $\rightarrow 6.7$ μs, where Δ is the chip width or spacing. Referring to Fig. 5-b which illustrates the hypothetical response function, we observe that it differs from the actual response function of this signal in at least two respects. Firstly, the central response peak at the origin will be replicated at zero relative range at the Doppler ambiguity corresponding to Δ, namely $\lambda/2\Delta$, where λ is the radar wavelength. If this ambiguity falls within the clutter the desired target response will be swamped, and range cells to either side of the target will be filled with clutter returns. Suppose we select a radar frequency of 2 GHz, placing operation between L- and S-band. Then $\lambda = .15$ meter and $v_{AMB} = 11.2$ km/sec, which is safely out of the clutter.

The second discrepancy between the hypothetical and actual response functions is the one which fundamentally undercuts any attempt at suppressing clutter with significant range and doppler extent using the suppression region of a phase-coded response function. This discrepancy corresponds to the fact that, far from extending indefinitely in the doppler dimension as in Fig. 5-b, the suppression region has a doppler extent less than $1/N\Delta$, the doppler resolution of the signal. Figure 3-c illustrates

this. Thus rather than appearing as in Fig. 5-b, the suppression region looks more like that shown in Fig. 5-d. In the present example the doppler resolution is 11.2/32 = .3 km/sec, so the suppression region doesn't even reach the clutter in doppler, no less encompass it.

In summary, "special" properties of phase-coded signals can be taken advantage of for clutter suppression only when doppler differentials or extents are qualitatively "small." This will not be the situation encountered in re-entry.

APPENDIX

Of the codes used as examples in this report, a fair number are (or are derived from) so-called maximal length shift register codes. They are shift register codes because they can be generated by clocking bits out of one end of a shift register. The input to the shift register is the modulo-two sum of a selected subset of the bits contained in the previous state of the register. The codes are maximal length because this subset of bits, the "feedback" bits, has been chosen so that the output sequence does not repeat itself until all possible states of the register other than all zeros have occurred. Such a code is then characterized by a shift register length, a specification of the feedback bits, and the initial contents of the register, or initial "load." As an example, consider the situation shown in Fig. A-1, which defines our conventions.

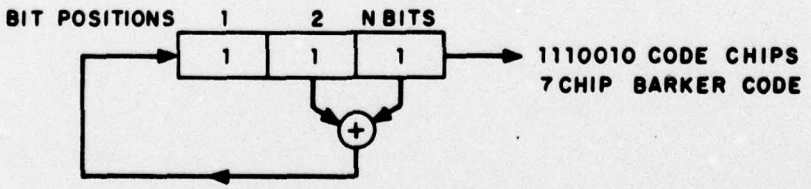

Fig. A-1. Generation of shift register code.

The register is NBITS long, 3 in this case. The initial load is 111, these bits filling the register from left to right. The register bits are indexed left to right from 1 to NBITS. The feedback bits are bits 2 and 3 in this case. One mod 2 adder is used here. It is equivalent to an exclusive OR operation on the two bits. More generally, more than two bits may be fed back. The number of bits fed back is even, and bit position NBITS is always included if the code is maximal length. If the set of feedback bits contains an odd number of 1's, the bit fed back is a 1. Otherwise it is a zero. The first NBITS chips of the phase code are the initial load bits in reverse order, and the length of the code is $2^{NBITS}-1$ chips. In this example, the code produced, or equivalently its complement, is the 7-chip Barker code. If any of the other possible $2^{NBITS}-2$ starting loads is used (all zeros is excluded), the code obtained is the original code cycled around. The autocorrelations of these other codes (6 in this example) will be different. If a different set of feedback bits is chosen, and the register length held fixed, a completely different set of codes will be generated, not necessarily maximal length.

With this background, Table A-1 summarizes the codes used in this memo which are either binary maximal length shift register codes or are derived from such. In addition, we used several codes that were not shift register derived. The first of these was Delong's 31 chip code[1] having lowest peak sidelobe (-20.3 dB) of any 31 chip

binary code. The code bits are

$$1000011010011111101010011101110 \quad .$$

As a check, the code in octal form should be 10323752356_8.

The other codes that were not shift register derived were the two 101 chip codes of Reference 2. These are represented below, where each row is read left to right and rows are read top to bottom.

(A) Sequence $\{a_n\}$

+ - - + +	- - + + +
+ + - + +	+ - + + -
+ + - + +	- + + - +
- - - - +	- - + - +
- + + + -	- + - + -
+ - + - +	- - - + +
+ + + + +	- + - - -
- - - + +	+ + - - -
- + + + +	- - - + +
+ + - - +	+ + - - +
+	

(B) Sequence $\{b_n\}$

+ - - + -	- - + + +
- - - + -	+ - - + -
+ + + + -	- + - + -
- + + - +	- + - + +
+ + - + -	- - - - +
+ - + + +	- - + + -
+ + - - -	+ - - - +
- - + - +	- + + + +
+ + + + +	+ + + - -
+ + - + -	- + + - -
+	

TABLE A-1

SHIFT REGISTER AND RELATED CODES

NCHIPS Code Length	Shift Register Length	Feedback Bit Positions	Initial Load Bits	Alterations	Remarks
31	5	2,3,4,5	01010 $=12_8$		Lowest Peak Sidelobe of any 31 chip shift register code.
32	5	3,5	11000 $=30_8$	Chip 1 Repeated as Chip 32	30 dB Peak Trench Level $\pm$6 Chips in Range
255	8	3,5,7,8	10001010 $=212_8$		40 dB Peak Trench Level $\pm$19 Chips Long.
1023	10	3,10	1000111000 $=1070_8$		50 dB Peak Trench Level $\pm$21 Chips Long.

ACKNOWLEDGMENT

Good typing support was provided by Kathleen O'Connell.

REFERENCES

1. D. F. Delong, "Experimental Autocorrelation of Binary Codes," Group Report 47G-0006, Lincoln Laboratory, M.I.T. (24 October 1960).

2. U. Somaini, "Binary Sequences with Good Autocorrelation and Cross Correlation Properties," IEEE Trans. Aerospace Electron. Systems AES-11, 1226 (1975).

3. F. E. Nathanson, Radar Design Principles (McGraw-Hill, New York, 1969).

4. K. S. Schneider and R. S. Orr, "Aperiodic Correlation Constraints on Large Binary Sequency Sets," IEEE Trans. Inf. Theory IT-21, 79 (1975).

(14) TN-1978-7

UNCLASSIFIED

SECURITY CLASSIFICATION OF THIS PAGE *(When Data Entered)*

(19) **REPORT DOCUMENTATION PAGE**

READ INSTRUCTIONS BEFORE COMPLETING FORM

(18) 1. REPORT NUMBER ESD-TR-78-30	2. GOVT ACCESSION NO.
3. RECIPIENT'S CATALOG NUMBER	
4. TITLE *(and Subtitle)* (6) Some Results on Phase-Coded Waveforms with Application to Reduction of Interference Between Radars	5. TYPE OF REPORT & PERIOD COVERED (9) Technical Note
	6. PERFORMING ORG. REPORT NUMBER Technical Note 1978-7
7. AUTHOR(s) (10) Dennis H. Pruslin	8. CONTRACT OR GRANT NUMBER(s) (15) F19628-78-C-0002
9. PERFORMING ORGANIZATION NAME AND ADDRESS Lincoln Laboratory, M.I.T. P.O. Box 73 Lexington, MA 02173	10. PROGRAM ELEMENT, PROJECT, TASK AREA & WORK UNIT NUMBERS (16) Project No. 8X363304D215
11. CONTROLLING OFFICE NAME AND ADDRESS Ballistic Missile Defense Program Office Department of the Army 5001 Eisenhower Ave. Alexandria, VA 22209	12. REPORT DATE (11) 28 Feb 1978
	13. NUMBER OF PAGES 54 (12) 52p
14. MONITORING AGENCY NAME & ADDRESS *(if different from Controlling Office)* Electronic Systems Division Hanscom AFB Bedford, MA 01731	15. SECURITY CLASS. *(of this report)* Unclassified
	15a. DECLASSIFICATION DOWNGRADING SCHEDULE

16. DISTRIBUTION STATEMENT *(of this Report)*

Approved for public release; distribution unlimited.

17. DISTRIBUTION STATEMENT *(of the abstract entered in Block 20, if different from Report)*

18. SUPPLEMENTARY NOTES

None

19. KEY WORDS *(Continue on reverse side if necessary and identify by block number)*

phase code
pseudo-random signals
shift register codes
autocorrelation
cross-correlation
radio frequency interference (RFI)
clutter suppression
ambiguity function

20. ABSTRACT *(Continue on reverse side if necessary and identify by block number)*

Some results on autocorrelation and cross-correlation properties of binary phase-coded radar waveforms are presented. The results are applied to a consideration of RFI reduction between radars and to questions of clutter suppression capability.

DD FORM 1 JAN 73 1473 EDITION OF 1 NOV 65 IS OBSOLETE

UNCLASSIFIED

SECURITY CLASSIFICATION OF THIS PAGE *(When Data Entered)*

207 65¢ JOB